

Ultra-small-angle neutron scattering: A tool to study packing of relatively monodisperse polymer spheres and their binary mixtures

Philip A. Reynolds,¹ Duncan J. McGillivray,^{1,2,*} Andrew J. Jackson,^{3,4} and John W. White¹

¹*Research School of Chemistry, The Australian National University, Canberra, Australian Capital Territory 0200, Australia*

²*Department of Chemistry, The University of Auckland, Auckland 1142, New Zealand*

³*NIST Center for Neutron Research, National Institute of Standards and Technology, Gaithersburg, Maryland 20899, USA*

⁴*Department of Materials Science and Engineering, University of Maryland, College Park, Maryland 20742, USA*

(Received 28 October 2008; revised manuscript received 12 May 2009; published 1 July 2009)

We measured ultra-small-angle neutron scattering (USANS) from polymethylmethacrylate spheres tamped down in air. Two slightly polydisperse pure sphere sizes (1.5 and 7.5 μm diameters) and five mixtures of these were used. All were loose packed (packing fractions of 0.3–0.6) with nongravitational forces (e.g., friction) important, preventing close packing. The USANS data are rich in information on powder packing. A modified Percus-Yevick fluid model was used to parametrize the data—adequately but not well. The modifications required the introduction of small voids, less than the sphere size, and a parameter reflecting substantial deviation from the Percus-Yevick prediction of the sphere-sphere correlation function. The mixed samples fitted less well, and two further modifying factors were necessary. These were local inhomogeneities, where the concentration of same-size spheres, both large and small, deviated from the mean packing, and a factor accounting for the presence within these “clusters” of self-avoidance of the large spheres (that is, large spheres coated with more small spheres than Percus-Yevick would predict). The overall deviations from the hard-sphere Percus-Yevick model that we find here suggest that fluid models of loose packed powders are unlikely to be successful but lay the ground work for future theoretical and computational works.

DOI: [10.1103/PhysRevE.80.011301](https://doi.org/10.1103/PhysRevE.80.011301)

PACS number(s): 45.70.-n, 61.05.fg, 61.43.Bn, 61.43.Gt

I. INTRODUCTION

A. Context and purpose

The packing of spheres is an immense, venerable, and active area of research; the general context of which can be found in the recent paper of Agnolin and Roux [1]. Our interest is particularly in the factors affecting the formation, the rheology, and the stability of highly concentrated emulsions, which are not well known. The nanometer scale structures of such emulsions—micelles and adsorbed surfactant monolayers—have been studied by small angle neutron scattering (SANS) [2–7]. We have also performed ultra-small-angle neutron scattering (USANS) experiments to give information on the micrometer-scale structures from a variety of emulsions [8]. These scattering curves contain useful information about droplet size distribution and correlations, but current sphere packing models do not extend to such high packing fractions (90–95 %) of such polydisperse particles.

To examine approximations that may be useful in modeling high packing fraction emulsion data, we have begun experiments on simpler assemblies of spherical beads. For beads and powders in the micrometer size range the results from larger sphere sizes cannot be scaled, as frictional and electrical forces become comparable to gravitational and substantially modify structures. Here we present results from relatively monodisperse polymer spheres of micrometer diameter and their binary mixtures in air at measured packing fractions from about 0.3–0.6. Such small jamming thresholds may be surprising; but aside from the experimental evidence, recent theory has shown that in tunneled crystals packing fractions as low as 0.49 can be obtained [9].

Agnolin and Roux [1] point out that information-rich experimental observation of packing microstructure has been difficult, and that experimental observations are required if we are to understand how closely numerical simulations resemble real-life systems. X-ray microtomography has been used to study the packing of large numbers of glass and acrylic beads in great detail [10–13], but small spheres cannot be studied because the resolution is limited to 30–60 μm . Confocal microscopy can be used for smaller spheres in emulsions, and glass beads, since it has a resolution of about 1 μm [8,14,15] but has the disadvantage of sampling very small volumes within the sample. Moreover, images cannot readily be resolved deep enough within the sample to unambiguously avoid edge effects.

USANS experimental results on packed spheres are presented in this paper. They show that USANS is a useful technique for examining micron-scale sphere packing, with results that are information rich. USANS spans the length ranges of approximately 0.5–20 μm and samples the bulk material with scattering arising from relatively large illuminated volumes. A modified Percus-Yevick fluid model, with a number of empirical adjustable parameters, is used to fit the data and shows that useful discrimination between different packing models may be possible with USANS. In subsequent work we hope to provide more satisfactory models, ideally using computational simulations.

B. Previous work

Previous experiments have been performed on micrometer or nanometer scale assembly of colloids [16–19], alloys [20], and powders [21–23] using USANS [16], ultra-small angle x-ray scattering [24], SANS [19], and small angle

*Corresponding author; d.mcgillivray@auckland.ac.nz

x-ray scattering [17,18], as well as many other techniques [21,22,25–27]. The appropriate fluid scattering models have been successfully fitted to monomodal concentrated oil-in-water emulsions [16], monomodal, bimodal, and trimodal Stober colloidal silica particles [17,24]; monomodal [18,26] and bimodal [25,27] concentrated latex or other polymer colloids; and dilute bimodal polymer colloid mixtures [19]. All except Sztucki *et al.* [24] do not need to invoke any force other than simple hard-sphere repulsion. Sztucki *et al.* also invoke a short-range hard-sphere stickiness.

Our experiments involve micrometer-scale polymer powder mixtures in air. Relevant simulation and packing fraction experiments show that similar powders are structured by highly significant nongravitational forces, as well as gravitation [28–30]. There have also been many computer simulations including size-polydisperse hard-sphere packing [31] and the voids within them [32]. Particularly relevant here are discussions of voids in loose packed powders [22,33]. From all these results, it seems clear that polymer spheres of 1–10 μm diameter will loose pack, with packing fractions of up to half the random close packing value of about 0.65, and will contain substantial amounts of void space. This is because electrical and frictional forces are significant compared to gravity. In contrast with the colloid experiments mentioned above, the models used to fit those data will not, as we will demonstrate below, fit our data. The colloid data also contrast with large hard-sphere packing in which gravity is dominant, for spheres of tenths of millimeter diameter or larger. This is where most experimental and theoretical activities have been concentrated [1,10–13,15,34–42]. Packing fractions exceed 0.55, and again the simplest fluid models, such as the Percus-Yevick, are inadequate, although bearing a resemblance to simulation results [36]. The best models, unfortunately, become empirical.

Various theories have been developed to explain the scattering from moderately concentrated assemblies of spheres. The simplest relatively realistic solutions involve spheres with Schulz size polydispersity, modeled as a fluid using the Percus-Yevick closure condition. These fit the colloid data relatively well, but not large hard-sphere experimental data. Exact analytical solutions for the scattering have been published by Griffith *et al.* for a monomodal distribution [43], Ginoza and Yasutomi for a bimodal “mixture” [44], and independently by Vrij [45] and Blum and Stell [46] a numerical solution for an arbitrary size distribution. There are various approximations or simplifications to these that have been published, notably Ashcroft and Langreth’s exact solution to the scattering from a binary mixture of monodisperse particles [23]. In addition Kotlarchyk and Chen [47] published an approximate theory, the “decoupling approximation,” separating intensity into a product of sphere self-scattering (form factor) and sphere-sphere interference (structure factor), together with useful averages such as the average sphere form factor of particles with a Schulz polydispersity. We apply these theories to our data to show that, unlike colloids, but like large hard spheres, assemblies of small hard spheres require more complex theories than those based on the Percus-Yevick model to explain their structure. Where the spheres are subjected to frictional forces in addition to grav-

ity, different structures *with the same packing fraction* become likely, with the differences dependent on sample history [1]. Packing fractions become smaller than equilibrium or metastable values [39].

II. EXPERIMENT

A. Polymer spheres and sample preparation method

We used two samples of dry polymer microspheres obtained from Bangs Laboratories Inc. (Indiana). They were fabricated from a mixture of 95% polymethylmethacrylate (PMMA) and 5% polydivinylbenzene (by mass) and had a hydrophilic sulfate ion surface coating. The specifications quote the density of the bulk polymer mixture as 1.19 g mL^{-1} . The producer stated values are 1.5(2) and 9.9(14) μm for the mean diameter of the spheres, with the estimated standard error given in parentheses. Samples containing 100%, 80%, 70%, 60%, 50%, 40%, and 0% of the larger sphere, by mass, and complementary amounts of smaller sphere were weighed out, and thoroughly macroscopically mixed, using a vortex mixer and grinding in a mortar and pestle.

B. USANS experiments

Samples were prepared by filling the cell with the pre-mixed microsphere mixture and tamped by firmly knocking the cell downward onto a horizontal surface until there was no more change in the level of the sample at the top of the cell. The density of material tamped in a similar way in cylindrical glass containers was measured volumetrically to give a powder packing fraction.

The USANS experiments were performed using the BT5 thermal neutron double-crystal instrument at the National Institute of Standards and Technology Center for Neutron Research, MD, USA [48]. 1-mm-thick samples were run for between 6 and 8 h each in quartz-windowed cells at a neutron wavelength of 2.4 \AA . Transmissions were high, always greater than 58%. The Q -dependent scattered beam intensity was always less than 20% and mostly less than 10% of the incident intensity. With these low values multiple scattering can be, and has been, neglected.

The scattering vector \mathbf{Q} is defined as the difference between the incident and the scattered neutron wave vectors. For elastic scattering, $Q=|\mathbf{Q}|=4\pi \sin \theta/\lambda$, where 2θ is the angle through which neutrons are scattered and λ is the neutron wavelength. A background from an empty beam run was subtracted from all the data, and the subtracted data processed to an absolute scale using the “straight through” beam intensities. A typical run allowed measurements with $3 \times 10^{-5} < Q_h < 5 \times 10^{-2} \text{ \AA}^{-1}$, where Q_h is the wave-vector component in the horizontal plane. This corresponds to probing length scales from 0.15 to 20 μm . The instrument has a vertical line beam profile extended in the vertical direction corresponding to a Q_v of maximum of $\pm 0.117 \text{ \AA}^{-1}$. The observed beam intensity at any nominal Q_h is thus a convolution of a range of actual Q . It is possible to desmear the observed data in order to simulate what would be seen by a pinhole beam method, with excellent resolution in both

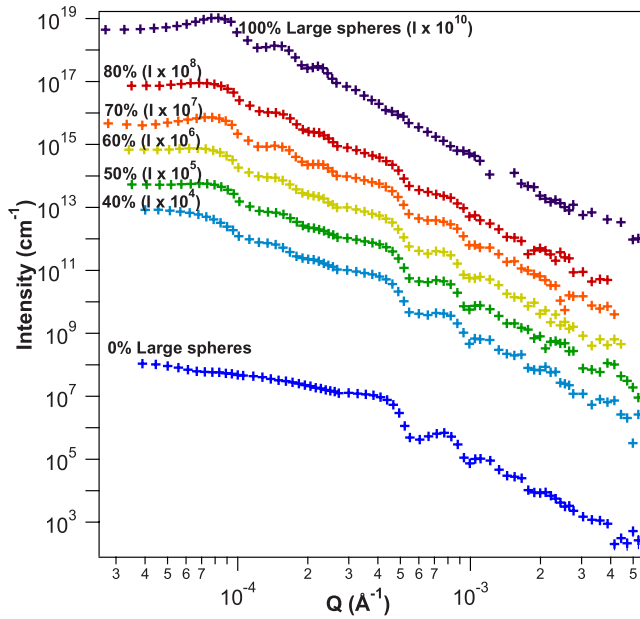


FIG. 1. (Color online) Desmeared USANS data from sphere mixtures. 0% large sphere data (=100% small spheres) are plotted on absolute scale; subsequent plots are displaced upward by (percentage large sphere)/10 decades. Thus for 50% large spheres the intensity plotted is 10^5 times experimental value. Error bars are within points except at highest Q .

planes. This desmearing can be performed by direct noniterative methods [49]. While the solutions are not unique, they are known to be reliable when used with caution. The results are shown in Fig. 1.

III. DATA ANALYSIS

The results of Yu *et al.* [29,30] imply that in our case we will require corrections to account for the change in sphere-sphere correlation from a Percus-Yevick fluid. These are caused by void formation, or conversely clustering, as a result of sphere-sphere attraction. In addition we are often working at packing fractions greater than 0.4 where it is known that the Percus-Yevick approximation gradually fails [50,51]. It is also clear from previous results, and preliminary modeling of our own, that we cannot neglect the effect of particle size polydispersity, even when, as here, it is quite narrow [43].

A. Unmixed spheres

Given that a complete, satisfactorily accurate, and simple model is unlikely, we will proceed in steps. First, we can estimate the invariant and Porod constants from the USANS data and from them produce model-independent estimates of packing fractions and scattering length densities [8,51]. If we assume monodispersity of spheres, we derive packing fractions of 0.45 and 0.61 for the smaller and the larger sphere samples. The scattering length densities derived from the data are 1.17×10^{-6} and $1.24 \times 10^{-6} \text{ \AA}^{-2}$. These are close to the value of $1.10 \times 10^{-6} \text{ \AA}^{-2}$ calculated from the formulas and the bulk density of the constituent polymers.

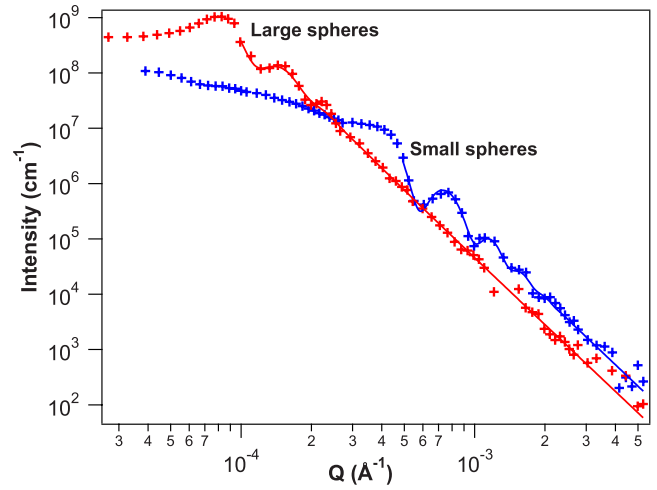


FIG. 2. (Color online) Fit of uncorrelated sphere model to only the high Q scattering data from samples of unmixed large spheres (red online) and unmixed small spheres (blue online).

Second, we can assume that at high Q the sphere-sphere structure factors will be close to unity and that the features in the USANS data will arise solely from the average spherical form factor over each Schulz particle size distribution, $\langle P_S(Q) \rangle$ and $\langle P_L(Q) \rangle$, where the subscripts S and L refer to small and large spheres. This fit is shown in Fig. 2. The scattering length densities were fixed at the values obtained from the invariant/Porod analysis, so the fitted packing fractions also closely resemble those values, differing slightly because we now account for polydispersity in the spheres. We obtain mean sphere diameters of $1.528(2) \mu\text{m}$ and $7.540(4) \mu\text{m}$, with polydispersities of 0.085(1) and 0.144(1), and with packing fractions 0.440(3) and 0.685(1).

We have found that we require two corrections to provide a good fit to all the data. The first is a correction for the persistence of voids in the sample and uses the Debye-Buche approximation for changes in the sphere-sphere correlation function or structure factor [24,33,52]. This we write as a Lorentzian correction,

$$S_{\text{DB}}(Q) = A_0 / (1 + Q^2 \zeta^2)^2, \quad (1)$$

where the packing-fraction-dependent parameters A_0 and ζ give, respectively, the total volume of void and void size (ζ is, more precisely, the correlation length of the void). Information on voids in powders is scarce [10,22,32,33,39]. Richard *et al.* [10] showed experimentally that the voids in their 200–400 μm glass bead system are almost all smaller than the sphere diameter and have a wide distribution of sizes depending on the amount of compaction. Our model of spherical smooth surfaced voids of air contrasted against a uniform background is oversimplified as the surface is not truly smooth. Also the uniform background has the averaged scattering length density of packed spheres with air interstices. Given the complexity there, and lack of knowledge, a more detailed model than the Debye-Buche correction seems unwarranted.

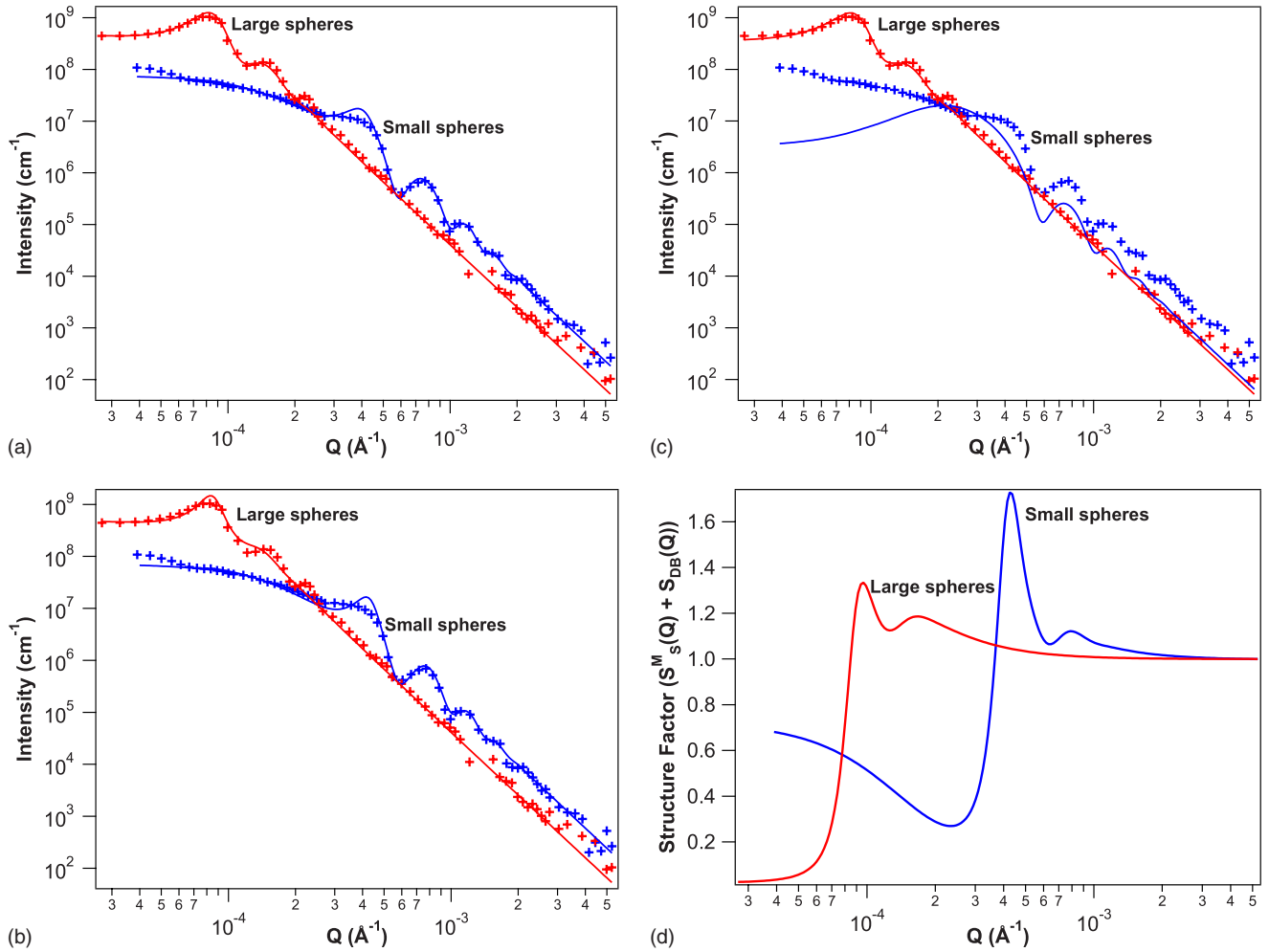


FIG. 3. (Color online) (a) Fit to the modified fluid model for unmixed large and unmixed small spheres (as labelled). (b) Fit to the modified fluid model to scattering data from unmixed spheres, omitting Debye-Buche void correction. Data from unmixed large spheres and unmixed small spheres are as labelled on the graph. (c) Fit to the modified fluid model to scattering data from unmixed spheres, including the Debye-Buche void correction but using only a single polydispersity parameter (i.e., $p_S=q_S$). Data from unmixed large spheres and unmixed small spheres are as labelled on the graph. (d) The total measurable structure factor [$S_S^M(Q)+S_{DB}(Q)$] from the best fit model plotted in Fig. 3(a), for small and large unmixed spheres (as labelled).

The second correction is necessary as we find that the usual Percus-Yevick fluid model for the scattering intensity does not fit well. A much better fit is obtained if we use a separated “measurable structure factor,” $S_{SS}^M(Q)$, and “mean form factor” $\langle P_S(Q) \rangle$, both defined in the Appendix. Each has a separate adjustable polydispersity, p and q respectively. Finally the packing fraction and scattering length density have been fixed at the values derived from the invariant/Porod analysis. This model then contains five parameters, sphere diameter (d) and polydispersity (p), structure factor polydispersity (q), and the two void parameters (A_0 and ζ). The fitting is shown in Fig. 3(a), while the parameters are given in Table I. We should note that the very small standard errors of about 1 part in 10^4 in Table I for the diameters are underestimated because the systematic errors in Q and intensity, while small, have not been factored into the analysis. The impact of the two corrections applied can be seen in Figs. 3(b) and 3(c). Figure 3(b) shows the results of fitting while omitting the Debye-Buche correction for voids, but with p_S and q_S varying independently. The correction has

little effect at high Q , or on the Porod constant, or invariant. Thus the preliminary analysis based on the latter two is little affected. Figure 3(c) shows the results of constraining p_S to equal q_S that is having a Percus-Yevick fluid perturbed only by the void Debye-Buche correction. Figure 3(d) shows the total measurable structure factor [$S_{SL}^M(Q)+S_{DB}(Q)$] derived from the best-fit model.

TABLE I. Fitted model parameters for unmixed spheres using best-fit model. Estimated uncertainties are given in parentheses.

Parameter	Small sphere	Large sphere
Sphere diameter d (μm)	1.5210(1)	7.536(2)
Sphere polydispersity $p_{S/L}$	0.085(1)	0.144(1)
Structure factor polydispersity $q_{S/L}$	0.177(1)	0.251(1)
void size ζ (μm)	0.455(4)	1.6(1)
void amount A_0 (unscaled)	1.53(1)	0.00016(1)

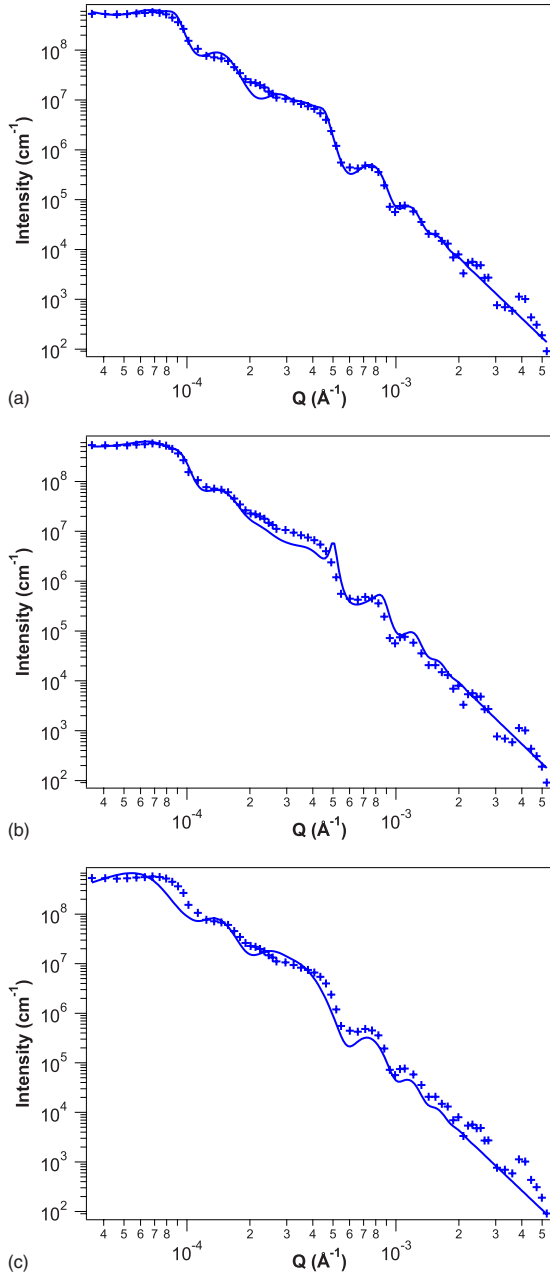


FIG. 4. (Color online) (a) Seven-parameter modified fluid model for mixed spheres (line) fit to the data from a mixture of 50% by mass each of large and small spheres. (b) Local monodisperse model for mixed spheres (line) fit to the data from a mixture of 50% by mass each of large and small spheres. (c) Seven-parameter model for mixed spheres with the amount of demixing set to zero (line) fit to the data from a mixture of 50% by mass each of large and small spheres.

B. Mixed spheres

The intensity of scattering from a system of mixed spheres is again modeled as consisting of void scattering and a modified Percus-Yevick fluid scattering, with the void scattering modeled by a Debye-Buche two-parameter expression generalized in an obvious way from the unmixed model. The unmodified analytical solution for a two-component Percus-Yevick fluid fits poorly. As with the one-component model-

TABLE II. Parameter values obtained for refinements of 50% data. Models named by related figure in which the derived fits are displayed. Estimated uncertainties are given in parentheses. “Fixed” denotes that the parameter was not allowed to vary in the modeling.

Parameter	4a	4b	4c
q_S	0.085(1)	0.085(1)	0.085(fixed)
q_L	0.153(2)	0.220(1)	0.153(fixed)
ζ (μm)	1.42(6)	1.42(fixed)	1.42(fixed)
A_0	0.273(3)	0.037(1)	0.035(6)
M	1.70(2)	0	2.33(1)
F	0.492(3)	0.193(1)	1
ϕ_S	0.259(1)	0.337(1)	0.166(1)
ϕ_L	$=\phi_S$	$=\phi_S$	$=\phi_S$

ing we have had to invoke a separate “structure factor polydispersity” parameter (q_S and q_L for small and large spheres). This requires the use of both one-component and two-component analytical solutions for the scattering. The total Percus-Yevick scattering is the sum of three terms, $I_{SS}(Q, \phi_L, \phi_S)$ —the scattering from interference between small spheres and small spheres and the corresponding large-large and large-small terms, as detailed in the Appendix. ϕ_L and ϕ_S are the volume fractions occupied by large and small spheres in the mixture. To provide better fits we also allow small-large sphere correlations to vary independently of self-correlations (large-large and small-small) using parameters M and F , respectively (see Appendix for details). This permits a balance of clustering not catered for in the Percus-Yevick model.

These various empirical approximations, required to obtain a reasonable fit, result in a large number of parameters needed to calculate the intensity. Some can be fixed from the unmixed data fits—sphere radii, sphere polydispersity, and particle scattering length density. We also know independently from the sample preparation the ratio of ϕ_L to ϕ_S . This leaves seven parameters to be fitted, two associated with the partial measurable structure factors (q_S and q_L), two with the Debye-Buche void correction approximation (A_0 and ζ), the parameters M and F , and one for the total sphere packing fraction. The total packing fraction must be fitted as it is not precisely known, and as we have seen from the unmixed data may differ from the volumetric measurements. The two individual sphere packing fractions can be determined by constraining the ratio of ϕ_S/ϕ_L to that as made up.

The results of this fit to the 50% data are shown in Fig. 4(a). For comparison we can neglect the intensity of scattering from large-small sphere interference effects, by putting $M=0$, known as the local monodisperse approximation [53] [Fig. 4(b)]. Figure 4(c) shows the best fit to the data when F is set to 1 and M is allowed to vary. This assumes that our approximation for the mixed intensity is adequate and there is no phase separation of large and small spheres. The parameters resulting from the three approximations are given in Table II. Where the parameters are noted “fixed” attempts to allow variation resulted in unstable fits. This is because in the mixed data ζ is strongly correlated with q_L . These param-

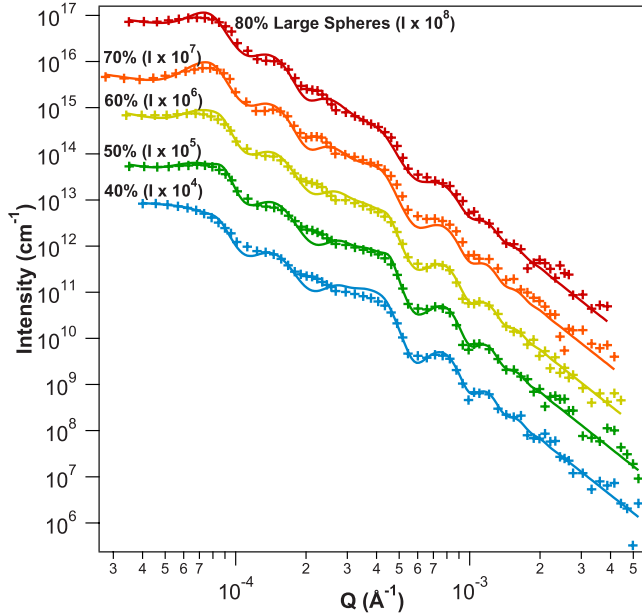


FIG. 5. (Color online) Desmeared USANS data from binary sphere mixtures, overlaid with best-fit modeled intensities. 0% large sphere intensities (not shown) are the experimental values, with subsequent plots displaced upward in intensity by (percentage large sphere)/10 decades. Thus for 50% large spheres the intensity plotted is 10^5 times experimental value. The model fits are the solid lines.

eters both affect only low Q data, a region that may be overparametrized.

It is possible to obtain an improved fit if we allow ϕ_L and ϕ_S to vary independently. This results in a packing fraction ratio strongly different from that in the mixture as made up. We consider this model as overparametrized.

The best model, illustrated in Fig. 4(a) for 50% large sphere data, is shown fitted to all the mixed data in Fig. 5 with the parameter values obtained given in Table III. To provide as unbiased an estimate of all the packing fractions, as we can from the USANS data, we have used the best models for all the data, *varying only the total packing fraction*, keeping all other parameters at their refined values. We restricted the data to those with $Q > 1 \times 10^{-3} \text{ \AA}^{-1}$. In this region we have almost no contribution from any variation in structure factor. The results are shown in Fig. 6.

TABLE III. Parameter values obtained for refinements of the mixed-sphere data. Estimated uncertainties are given in parentheses.

% large sphere (by mass)	80	70	60	50	40
q_S	0.085(1)	0.085(1)	0.085(1)	0.085(1)	0.085(1)
q_L	0.169(3)	0.164(2)	0.156(3)	0.153(2)	0.140(3)
ζ (μm)	0.05(3)	0.27(5)	0.73(3)	1.42(6)	1.3(1)
A_0	0.142(2)	0.177(3)	0.279(6)	0.273(3)	0.39(2)
M	3.81(6)	4.1(2)	1.77(3)	1.70(2)	1.80(3)
F	0.67(1)	0.47(1)	0.569(5)	0.492(3)	0.62(1)
ϕ_S	0.084(1)	0.125(1)	0.198(1)	0.259(1)	0.268(1)

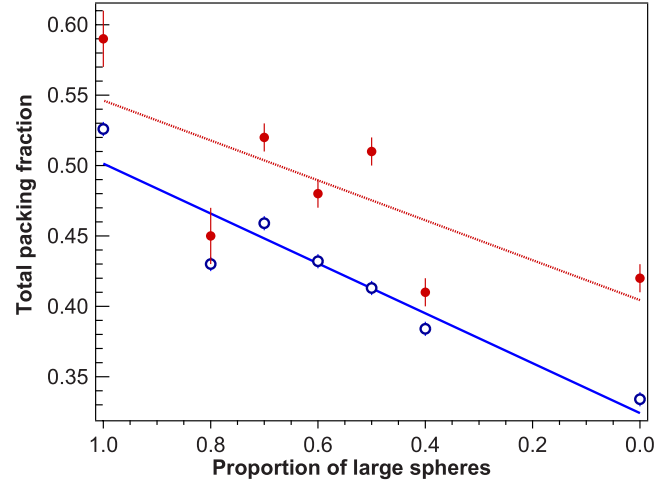


FIG. 6. (Color online) Total packing fraction in mixtures of large and small spheres measured volumetrically (hollow circles) and determined from USANS data (filled circles). The lines are best-fit linear regressions to the data.

IV. DISCUSSION

A. Packing fraction

The volumetrically measured total packing fraction varies from 0.334 for the pure $1.52 \mu\text{m}$ diameter spheres to 0.526 for the $7.54 \mu\text{m}$ diameter spheres. The packing fractions of the mixtures are intermediate between those values, declining in a linear trend with increasing small sphere proportion. The corresponding values derived from the USANS measurements, by adding together the small and large sphere packing fractions ϕ_S and ϕ_L , are higher [0.42(1) for the small spheres to 0.59(2) for the large spheres] and show larger variation from a linear trend (see Fig. 6). We should note that the USANS “packing fraction” does not include the contribution from voids modeled by the Debye-Buche correction and is thus a lower bound. The void contribution can be calculated from the parameters A_0 and ζ . The values calculated cluster around a reasonable value of 0.1, with errors of comparable size. This is because of the dependence of the value of the void packing fraction on the third power of ζ and systematic errors in the latter, which make a useful estimate from this model impossible. It is clear that a better model for voids, indeed the whole structure, is needed. The differences between the two techniques can best be attributed to variations in the tamping between the different containers and from sample to sample—in particular if the tamping from the “as poured” state to the “fully tamped” state is not fully accomplished and slightly variable. Yu *et al.* [30] measured the difference in packing fraction between these two states as about 0.15, almost independent of particle size, within the difference between the measurements.

All these values are well below the total packing fraction of about 0.65 expected for unmixed-sphere random close packing, with even higher values expected for binary mixtures. The role of nongravitational forces does appear important. If this is so, the smaller particles are expected to be less densely packed, as observed. Yu *et al.* [29,30], in both experiment on alumina powders and computer simulation,

found qualitatively similar effects—packing fraction of about 0.2 for 1 μm particles to 0.4 for 10 μm particles. We should not expect exact agreement given the differences in mechanical and electrical properties of the various particles, and that the computer simulation is closer to an as poured than fully tamped state.

B. Qualitative

For the pure small spheres we see the characteristic oscillations in intensity at high Q for relatively monodisperse spheres, with the oscillations shifted to lower Q larger spheres. At the lowest Q the large sphere data show a downturn in intensity, resembling that for a close packed fluid; but the data for the smaller spheres continue to increase. We can ascribe this to the larger deviation from close packed for the small spheres, as is also shown by the packing fractions in that case. This larger deviation from fluidlike scattering at low Q implies many more voids in the smaller sphere sample.

The mixed-sphere data at high Q , which show both oscillations, appears close to a weighted average of the pure sphere data. This is to be expected since these oscillations result from single-sphere/air interface scattering. The data at lower Q show scattering attributed to voids that are intermediate between the pure samples.

C. Model fits to unmixed spheres

The fit to the modified Percus-Yevick fluid model for the unmixed spheres is shown in Fig. 3(a). We notice a systematic deviation of the fit from the data in both plots. At high Q the oscillations due to the sphere morphology wash out too soon, while at the first peak the oscillation is too strong. If we contemplate the measurable structure factors plotted in Fig. 3(d), we notice the general resemblance to those for a typical fluid. However the nonempirical Percus-Yevick structure factor model is evidently not sufficiently flexible at lower Q , and the empirical factor, the sphere polydispersity factor (p_s), increases from its true value to attempt to compensate in the fit at low Q . Apart from this minor deficiency the model performs well. The values of the USANS packing fraction discussed above and the remaining parameters in Table I are not unreasonable. The derived value for the diameter of the small spheres agrees with the dynamic light scattering (DLS) value quoted by the manufacturer of the spheres, while the larger sphere derived diameter is 76% of the DLS value. In the large sphere case, however, the DLS value has a large stated uncertainty, equivalent to 14% of the diameter.

The significantly larger values in both cases for the structure factor polydispersity parameter than for the particle structure factor shows that the structure is far from a Percus-Yevick model fluid structure [illustrated in Fig. 3(c)]. We should not be surprised since at these packing fractions (0.4–0.6) the Percus-Yevick approximation is known to fail. The Debye-Buche void correction is highly significant for the small spheres, but less so for the large [Fig. 3(b)], in agreement with the higher achieved packing fraction. The void sizes refine to values smaller than the sphere diameters in

both cases, indicating that the structure does not resemble a fluid with spheres picked out, rather a fluid less efficiently packed than a true fluid. The derived measurable structure factors of Fig. 3(d) are reasonable, but given the caveats we have made above a first-principles computer simulation would be necessary to progress further in modeling.

D. Model fits to sphere binary mixtures

The fits for the mixed-sphere data are illustrated for the 50/50 mixture in Figs. 4(a)–4(c). Figures 4(b) and 4(c) illustrate that the parameters associated with imperfect mixing (F) and small-sphere large sphere structure factor correlations (M) are both significant. The lower overall quality of the fit in Fig. 4(a) compared to that for the unmixed spheres in Fig. 3(a) suggests that these factors are not perfectly described by our model.

We thus have three factors important in the mixed structure. We will call these “demixing,” “large-small correlation” and “voids,” of which only the last is present in the unmixed structures. Demixing is where the self-scattering terms $I_{SS}(Q, \phi_L, \phi_S)$ and $I_{LL}(Q, \phi_L, \phi_S)$ from the Percus-Yevick model are not adequate to describe these terms in the mixture, and we need to include terms $I_{SS}(Q, 0, \phi'_S)$ and $I_{LL}(Q, \phi'_L, 0)$, where ϕ'_S and ϕ'_L are the phase fractions for unmixed pure sphere volumes. For simplicity this three-phase model assumes that any demixing that occurs is complete—so that the three regions are completely unmixed small spheres, completely unmixed large spheres, and perfectly mixed spheres. Intermediate models where there are local clusters rich in large spheres and separate local clusters rich in small spheres are more physically appealing, but necessarily introduce more empirical parameters. In most cases the proportion of demixing required is large—about half of the sample being demixed to form unmixed regions.

Demixing will of course reduce the large-small correlation and thus $I_{SL}(Q, \phi_L, \phi_S)$. From the fit we see this change is resisted with M values refining to values greater than 1. Thus there is more large-small correlation than we would expect. If we accept the demixing, then we must conclude that in those local volumes of mixed spheres the large and small spheres are not randomly distributed. Large spheres tend to self-avoid and are coated by small spheres more than would otherwise be predicted.

Lastly voids in the mixed-sphere samples are smaller than the large spheres and increase in amount as the small sphere fraction increases. This is as we would naively expect, although there is no reason to expect a linear interpolation. As with gravity-dominated sphere mixing, where packing fraction peaks in the mixed-sphere region, more complicated factors may intervene. The large-small correlation factor shows mixtures are more than the sum of the parts.

Fantoni and Pastore [36] showed by Monte Carlo simulations that binary mixtures do show features not found in one-component systems. However Abate and Durian [42] found little experimental difference between the various large and small sphere correlations, apart from trivial size scaling. The optical experiments of Sun Sevick-Muraca [26] on colloids at lower packing fractions extract only one struc-

tural parameter per mixture, but do support the conclusion that large-small correlation is significant. These conflicts may be related to the ratio of radii between large and small spheres, respectively, 1.375 [42], 1.667 [36], 1.53 [26], and 4.955 in this work.

The x-ray scattering experiments on relatively concentrated silica particle colloids, both pure relatively monodisperse and binary mixtures [17,24], show good agreement with Percus-Yevick fluid models. This extends to packing fractions of 0.45, within the bounds of our experiments. The discussion in this paper is based on an assumption that a Percus-Yevick fluid solution is appropriate for these nonequilibrium samples of high volume fraction and complex sphere-sphere interaction. The relatively poor model fits for the mixed-sphere data throws doubt on this, and the x-ray data suggest that this is not due to the inaccuracy of the Percus-Yevick model due to high packing fractions, but to more fundamental physical causes—the sphere-sphere interaction potential is far from hard sphere, involving frictional and electrostatic forces. A way forward is to extend the computer simulation of Yang *et al.* [29] to mixtures, where these extra forces can be taken into account. Given the richness of the spectra this would seem profitable.

V. CONCLUSIONS

The USANS from unmixed small (1.5 mm diameter) and large (7.5 mm diameter) PMMA spheres can be fitted by a hard-sphere Percus-Yevick fluid model, which requires modification in two ways. This contrasts with relatively dilute emulsions in which a simple Percus-Yevick fluid model suffices [16]. The first modification is that a Debye-Buche scattering term must be added, representing a significant population of voids in the fluid with a void size that refines to about a quarter of the sphere size. Second, the sphere-sphere correlation function is not well fitted by using the polydispersity in sphere radius. We must allow this to vary independently for the form factors and the structure factors, so that the structure factor polydispersity is actually now an empirical factor allowing a better fit of the sphere-sphere correlation. The model represents a fluid slightly less uniformly packed than a true fluid. The packing fractions obtained compare well with those measured volumetrically and indicate loose packing with significant frictional and/or electrical forces compared to gravitational, particularly for the small spheres.

The USANS from mixtures of small and large spheres can be fitted to a related Percus-Yevick fluid model with Debye-Buche void correction, but not as satisfactorily, requiring further modifications to the model. We need to invoke two further empirical parameters to produce an acceptable fit, demixing, and large-small correlation parameters. The demixing parameter adjusts the scattering to replace some of the scattering from mixed spheres with that from volumes of pure unmixed spheres. This is a simple approximation, which does not account for the probable situation in which there are local clusters rich in large spheres and separate local clusters rich in small spheres. The large-small correlation parameter highlights this, in that it reflects that in the volumes of mixed

spheres large and small spheres are not randomly distributed. Large spheres tend to self-avoid and are coated in more small spheres than we would otherwise predict.

The model for mixed spheres is cumbersome because the mixed spheres do not resemble a Percus-Yevick fluid locally. The structure contains voids, local clusters deviating from the overall stoichiometry, and large-small sphere correlations which are larger than expected. The five empirical parameters that we introduced are really only modifying the low Q part of the data, so that the model is overparametrized in this region.

Nevertheless it is clear that the USANS data on powders contain nontrivial information relating to the packing, and that a simple fluid model, with added empirical parameters, can give physical insight into the system. A different theoretical approach, such as computer simulation, with fewer or no empirical parameters is called for to understand these effects more effectively.

ACKNOWLEDGMENTS

The USANS data were obtained using facilities supported in part by the National Science Foundation under Agreement No. DMR-045467. We acknowledge financial support from the Access to Major Research Facilities Programme, which is a component of the International Science Linkages Programme, established under the Australian Government's innovation statement, Backing Australia's Ability. D.J.M. gratefully acknowledges financial support from the Australian Institute of Nuclear Science and Engineering.

APPENDIX

1. Unmixed-sphere intensity

We write the intensity of scattering from small spheres, neglecting the void contribution as

$$I_{SS}(Q) = \phi_S \langle\langle V_S \rangle\rangle \langle\langle P_S(Q) \rangle\rangle S_{SS}^M(Q), \quad (A1)$$

where $\langle\langle V_S \rangle\rangle$ is the small sphere mean volume and $I_{SS}(Q)$ is calculated exactly [24], but using a variable structure factor polydispersity. The subscripts refer to large (L) and small (S) spheres. Thus we are using a different polydispersity for the mean form factor $\langle P_S(Q) \rangle$ (denoted as p_S) to that used to calculate $S_{SS}^M(Q)$ (denoted as q_S). Then when we use p_S in calculations and averages we write $\langle \rangle$ and when we use q_S we write $\langle\langle \rangle\rangle$ (and similarly for the large spheres).

We can then write the total intensity as

$$I_{SS}(Q) = \phi_S \langle\langle V_S \rangle\rangle \langle P_S(Q) \rangle [S_{SS}^M(Q) + S_{DB}(Q)]. \quad (A2)$$

The large sphere intensity is similarly approximated.

2. Mixed-sphere intensity

We will write a general equation for the observed intensity, $I(Q, \phi_L, \phi_S)$, in a single phase mixture as

$$I(Q, \phi_L, \phi_S) = I_{SS}(Q, \phi_L, \phi_S) + 2I_{SL}(Q, \phi_L, \phi_S) + I_{LL}(Q, \phi_L, \phi_S) + I_{DB}(Q, \phi_L, \phi_S). \quad (A3)$$

$I_{SL}(Q, \phi_L, \phi_S)$ is the scattering intensity derived from inter-

ference between large and small spheres whose packing fractions in the mixture are ϕ_L and ϕ_S . That is $(1 - \phi_L - \phi_S)$ is the packing fraction of air in the mixture. The terms $I_{SS}(Q, \phi_L, \phi_S)$ and $I_{LL}(Q, \phi_L, \phi_S)$ are obvious by analogy. The term $I_{DB}(Q, \phi_L, \phi_S)$ is used to account for the scattering arising from the formation of voids within the mixture. We now define each of these terms in more detail.

We choose to write $I_{DB}(Q, \phi_L, \phi_S)$ as

$$I_{DB}(Q, \phi_L, \phi_S) = [\langle P_S(Q) \rangle \phi_S + \langle P_L(Q) \rangle \phi_L] / (\phi_S + \phi_L) A_0 / (1 + Q^2 \xi^2)^2. \quad (\text{A4})$$

For mixtures this analytical form is the simplest of the many alternatives, which reduces to the approximation used for the unmixed spheres at the limit where either of ϕ_S and ϕ_L is equal to zero. It may be physically incorrect if, for example, void sizes in mixtures are strongly biased to the volume of the smaller particle.

The quantities $I_{SS}(Q, \phi_L, \phi_S)$, $I_{SL}(Q, \phi_L, \phi_S)$, and $I_{LL}(Q, \phi_L, \phi_S)$ are more difficult to define. The exact solutions for a Percus-Yevick bimodally Schulz polydisperse fluid [25–27] cannot be directly applied since we have shown above for the unmixed spheres that the sphere-sphere measurable structure factor is substantially damped from these calculated values.

For $I_{SS}(Q, \phi_L, \phi_S)$ [and similarly for $I_{LL}(Q, \phi_L, \phi_S)$] we can make the approximation

$$I_{SS}(Q, \phi_L, \phi_S) = \phi_S \langle \langle V_S \rangle \rangle \langle P_S(Q) \rangle S_{SS}^M(Q). \quad (\text{A5})$$

In a second approximation we write

$$I_{SL}(Q, \phi_L, \phi_S) = M(\phi_S \langle \langle V_S \rangle \rangle \langle P_S(Q) \rangle \phi_L \langle \langle V_L \rangle \rangle \times \langle P_L(Q) \rangle)^{1/2} \langle S_{SL}(Q) \rangle, \quad (\text{A6})$$

where $S_{SL}(Q)$ is the structure factor cross term calculated by the use of the monodisperse bimodal scattering theory of Ashcroft and Langreth [23]. $\langle S_{SL}(Q) \rangle$ is calculated by calculating $S_{SL}(Q)$ for all pairs of small and large sphere diameters and making a weighted average of these with the product of the appropriate Schulz sphere polydispersities. This is an attempt to account for sphere polydispersity. M is a variable allowing small-large sphere correlations to vary independently of large-large and small-small correlations.

Lastly we have found it necessary to modify these sphere-sphere correlations. We make the approximation

$$I = FI(\text{mixed}) + (1 - F)I(\text{unmixed}). \quad (\text{A7})$$

$I(\text{mixed})$ is $I(Q, \phi_L, \phi_S)$. $I(\text{unmixed})$ is the sum of the scattering from unmixed large and small sphere phases resulting from complete demixing of a proportion $(1 - F)$ of the sample. This approximation allows self-correlations, $I_{SS}(Q, \phi_L, \phi_S)$ and $I_{LL}(Q, \phi_L, \phi_S)$, to be modified to allow for clustering not catered for in the Percus-Yevick model.

-
- [1] I. Agnolin and J.-N. Roux, *Phys. Rev. E* **76**, 061302 (2007).
 [2] C. Solans, R. Pons, S. Zhu, H. T. Davis, D. F. Evans, K. Kamakura, and H. Kunieda, *Langmuir* **9**, 1479 (1993).
 [3] A. Langenfeld, F. Lequeux, M. J. Stebe, and V. Schmitt, *Langmuir* **14**, 6030 (1998).
 [4] P. A. Reynolds, E. P. Gilbert, and J. W. White, *J. Phys. Chem. B* **104**, 7012 (2000); this paper more completely references previous SANS data on emulsions.
 [5] P. A. Reynolds, E. P. Gilbert, and J. W. White, *J. Phys. Chem. B* **105**, 6925 (2001).
 [6] P. A. Reynolds, E. P. Gilbert, and J. W. White, *J. Phys. Chem.* (to be published).
 [7] K. J. Baranyai, P. A. Reynolds, M. J. Henderson, and J. W. White (unpublished).
 [8] K. J. Baranyai, P. A. Reynolds, A. J. Jackson, M. J. Henderson, J. Zank, J. G. Barker, M.-H. Kim, and J. W. White (unpublished).
 [9] S. Torquato and F. H. Stillinger, *J. Appl. Phys.* **102**, 093511 (2007).
 [10] P. Richard, P. Philippe, F. Barbe, S. Bourles, X. Thibault, and D. Bideau, *Phys. Rev. E* **68**, 020301(R) (2003).
 [11] M. Jerkins, M. Schroter, H. L. Swinney, T. J. Senden, M. Saadatfar, and T. Aste, *Phys. Rev. Lett.* **101**, 018301 (2008).
 [12] T. Aste, M. Saadatfar, and T. J. Senden, *Phys. Rev. E* **71**, 061302 (2005).
 [13] T. Aste, M. Saadatfar, A. Sekellariou, and T. J. Senden, *Physica A* **339**, 16 (2004).
 [14] J. Brujić, S. F. Edwards, I. Hopkingson, and H. A. Makse, *Physica A* **327**, 201 (2003).
 [15] M. M. Kohonen, D. Geremichalos, M. Scheel, C. Schier, and S. Herminghaus, *Physica A* **339**, 7 (2004).
 [16] C. P. Whitby, A. M. Djerdjev, J. K. Beattie, and G. G. Warr, *Langmuir* **23**, 1694 (2007).
 [17] B. J. Anderson, V. Gopalakrishnan, S. Ramakrishnan, and C. F. Zukoski, *Phys. Rev. E* **73**, 031407 (2006).
 [18] D. Lumma, L. B. Lurio, M. A. Borthwick, P. Falus, and S. G. J. Mochrie, *Phys. Rev. E* **62**, 8258 (2000).
 [19] R. H. Ottewill, A. R. Rennie, and G. D. W. Johnson, *Adv. Colloid Interface Sci.* **100-102**, 585 (2003).
 [20] J. F. Wax, N. Jakse, and I. Charpentier, *Physica B* **337**, 154 (2003).
 [21] P. S. Roller, *Ind. Eng. Chem.* **22**, 1206 (1930).
 [22] J. M. Valverde and A. Castellanos, *EPL* **75**, 985 (2006).
 [23] N. W. Ashcroft and D. C. Langreth, *Phys. Rev.* **156**, 685 (1967); **166**, 934 (1968).
 [24] M. Sztucki, T. Narayanan, G. Belina, A. Moussaid, F. Pignon, and H. Hoekstra, *Phys. Rev. E* **74**, 051504 (2006).
 [25] Z. Sun and E. M. Sevick-Muraca, *J. Colloid Interface Sci.* **270**, 329 (2004).
 [26] Z. Sun and E. M. Sevick-Muraca, *Langmuir* **18**, 1091 (2002).
 [27] B. E. Rodriguez and E. W. Kaler, *Langmuir* **8**, 2376 (1992).
 [28] K. Z. Y. Yen and T. K. Chaki, *J. Appl. Phys.* **71**, 3164 (1992).
 [29] R. Y. Yang, R. P. Zou, and A. B. Yu, *Phys. Rev. E* **62**, 3900 (2000).
 [30] A. B. Yu, J. Bridgewater, and A. Burbidge, *Powder Technol.* **92**, 185 (1997).

- [31] A. Yang, C. T. Miller, and L. D. Turcoliver, *Phys. Rev. E* **53**, 1516 (1996).
- [32] G. T. Nolan and P. E. Kavanagh, *Powder Technol.* **78**, 231 (1994).
- [33] S. R. Bhatia, *Curr. Opin. Colloid Interface Sci.* **9**, 404 (2005).
- [34] H. J. H. Brouwers, *Phys. Rev. E* **74**, 031309 (2006).
- [35] Ph. Germain and S. Amokrane, *Phys. Rev. E* **76**, 031401 (2007).
- [36] R. Fantoni and G. Pastore, *J. Chem. Phys.* **120**, 10681 (2004).
- [37] G. N. Sarkisov, *J. Chem. Phys.* **119**, 373 (2003).
- [38] D.-M. Duh and A. D. J. Haymet, *J. Chem. Phys.* **103**, 2625 (1995).
- [39] M. D. Rintoul and S. Torquato, *Phys. Rev. E* **58**, 532 (1998).
- [40] M. D. Rintoul and S. Torquato, *J. Chem. Phys.* **105**, 9258 (1996).
- [41] A. R. Abate and D. J. Durian, *Phys. Rev. Lett.* **101**, 245701 (2008).
- [42] A. R. Abate and D. J. Durian, *Phys. Rev. E* **74**, 031308 (2006).
- [43] W. L. Griffith, R. Triolo, and A. L. Compere, *Phys. Rev. A* **33**, 2197 (1986).
- [44] M. Ginoza and M. Yasutomi, *Phys. Rev. E* **59**, 3270 (1999).
- [45] A. J. Vrij, *J. Chem. Phys.* **71**, 3267 (1979).
- [46] L. Blum and G. J. Stell, *J. Chem. Phys.* **71**, 42 (1979).
- [47] M. Kotlarchyk and S. H. Chen, *J. Chem. Phys.* **79**, 2461 (1983).
- [48] A. R. Drews, J. G. Barker, C. J. Glinka, and M. Agamalian, *Physica B* **241-243**, 189 (1997).
- [49] M. A. Singh, S. S. Ghosh, and R. F. Shannon, *J. Appl. Crystallogr.* **26**, 787 (1993).
- [50] P. A. Egelstaff, *An Introduction to the Liquid State* (Academic Press, London, 1967).
- [51] *Neutrons, X-Rays and Light: Scattering Methods Applied to Soft Condensed Matter*, edited by P. Lindner and Th. Zemb (North Holland, Amsterdam, 2002).
- [52] P. Schmidt, in *Modern Aspects of Small Angle Scattering*, edited by H. Brumberger (Kluwer Academic, Dordrecht, 1995), p. 1.
- [53] J. S. Pedersen, *J. Appl. Crystallogr.* **27**, 595 (1994).